

# CHARACTERIZATION OF ROUGH FRACTAL SURFACES FROM BACKSCATTERED RADAR DATA

A. Kotopoulis, G. Pouraimis, A. Malamou, E. Kallitsis and P. Frangos

National Technical University of Athens  
9, Iroon Polytechniou Str., GR 157 73, Zografou, Athens, Greece

Tel: +30 210 772 3694, Fax: +30 210 772 2281, E-Mail: pfrangos@central.ntua.gr

## Abstract

In this paper the scattering of electromagnetic (EM) waves, emitted by a monostatic radar, from rough fractal surfaces is examined by using the Kirchhoff approximation. We examine here the way that the level of roughness of the fractal surface affects the backscattered EM wave captured by a radar as a function of frequency (therefore, a 'spectral method'), and whether the roughness of the surface can be estimated from these radar measurements. The backscattering coefficient is calculated for a number of radar frequencies and for different values of the surface fractal dimension. It is found here that the values of the slopes between the main lobe and the first sidelobes of the backscattering coefficient as a function of the wavenumber (frequency) of the incident EM waves increase with the surface fractal dimension. Therefore, we conclude that the magnitude of the above slopes provides a reliable method for the classification of the rough fractal surfaces. The above are also investigated in the presence of electronic noise in the radar receiver (effect of SNR values in the above proposed technique).

## 1. INTRODUCTION

The scattering of electromagnetic (EM) waves from rough surfaces has been for decades a very interesting subject for scientific investigation. In many cases the main purpose of this research is the characterization of rough surfaces from scattered EM wave data for remote sensing applications, in the microwave or optical regime [1]–[16]. These surfaces can be modelled mathematically with deterministic or random functions [1]–[3]. However, introducing the fractal geometry, these surfaces can be described in a more detailed way in multiscale [1], [3], [8], [17].

In this paper the scattering of EM waves from rough surfaces using the Kirchhoff approximation is examined [1], [2]. In particular, in Section II the mathematical fundamentals for scattering of EM waves from fractal surfaces are summarized [1]–[3].

In Section III our simulation results for the characterization of the rough fractal surfaces from backscattered EM wave data are presented. Finally, conclusions and future related research of ours are described in Section IV.

## 2. PROBLEM GEOMETRY AND MATHEMATICAL FORMULATION

The geometry of the problem is shown in Fig. 1. An incident EM plane wave illuminates a one – dimen-

sionally rough fractal surface extending from  $x = -L$  to  $x = L$ , as shown in Fig. 1. The angle of incidence of the EM wave is  $\theta_i$  with respect to the vertical  $z$  axis, where the incident and scattered wave vectors are denoted by  $\mathbf{k}_i$  and  $\mathbf{k}_s$  respectively [1].

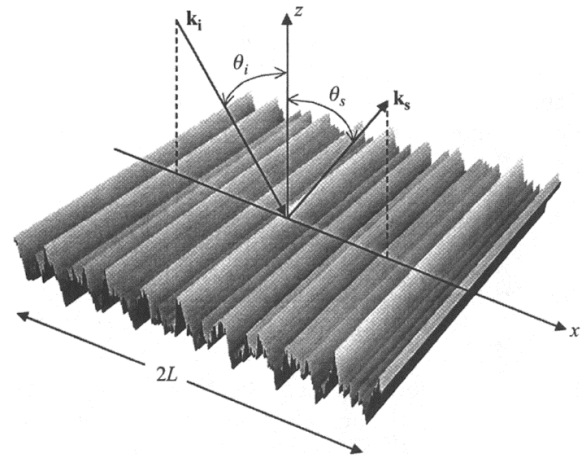


Fig. 1. Geometry of rough surface scattering problem in which an incident plane wave illuminates a fractal surface patch of size  $2L$  at an angle  $\theta_i$

Following [1], and in order to describe the surface roughness, a one-dimensional fractal function is used [1], [3], [4]. This fractal function is described by the following equation:

$$f_r(x) = \sigma C \sum_{n=0}^{N-1} (D-1)^n \sin(K_0 b^n x + \phi_n) \quad (1)$$

where  $D$  ( $1 < D < 2$ ) is the fractal dimension of fractal surface [1],  $K_0 = 2\pi/\Lambda_0$  is the fundamental spatial wavenumber of the fractal surface,  $\Lambda_0$  is the corresponding fundamental spatial wavelength,  $b$  (where  $b > 1$ ) is the spatial frequency scaling parameter,  $\phi_n$  are arbitrary phases and  $N$  is the number of tones describing the surface. The amplitude control factor  $C$  is given by

$$C = \left\{ \frac{2D(2-D)}{[1-(D-1)^{2N}]} \right\}^{\frac{1}{2}} \quad (2)$$

so that surface function (1), has standard deviation (rms height) equal to  $\sigma$  (see [1]). It can be easily realized from (1) above, that when the surface fractal dimension  $D$  increases from value 1 to value 2, the surface roughness also increases (see [1], [3] for more details).

In order to calculate the scattered field from a rough fractal surface, as described in Fig. 1, the Kirchhoff approximation is used in this paper, for which it is assumed that the wavelength of the incident EM wave is small compared to the local radius of curvature of the surface roughness [1]–[3]. Furthermore, for the plane EM wave incidence of Fig. 1, in [1] it is shown that the scattered electric field is given by the following equation:

$$E_{sc} = \frac{ikL \exp(ikR_0)}{2\pi R_0} \int_{-L}^L (pf'_r - q) \exp[iv_x x + iv_z f_r(x)] dx \quad (3)$$

where

$$p = (1 - R) \sin \theta_i + (1 + R) \sin \theta_s \quad (4)$$

$$q = (1 + R) \cos \theta_s - (1 - R) \cos \theta_i \quad (5)$$

$$v_x = k(\sin \theta_i - \sin \theta_s) \quad (6)$$

$$v_z = k(\cos \theta_i + \cos \theta_s) \quad (7)$$

In the above (3)–(7)  $R_0$  is the distance from the observation point (monostatic radar) to the origin, coinciding with the 'source surface point',  $k$  is the wavenumber of the incident EM wave ( $k=2\pi f/c$ , where  $f$  is the frequency of the incident EM wave),  $R$  is the Fresnel reflection coefficient of the tangential plane at the point of interest,  $\theta_s$  is the direction of the observer and  $f'_r$  is the derivative with respect to its argument ( $x$ ). For simplicity we assume a perfectly conducting rough surface, in which case the Fresnel reflection coefficient is given by ( $R^+ = 1$ ,  $R^- = -1$ ), where the superscript + indicates the paral-

lel (vertical) polarization and the superscript – denotes the perpendicular (horizontal) polarization, respectively [1], [2].

In the case of a smooth and perfectly conducting surface, the scattered field for horizontal polarization can be found in the direction of specular reflection, namely for  $\theta_i = \theta_s$  [1], [2]:

$$E_{sc0} = \frac{i2kL^2 \exp(ikR_0) \cos \theta_i}{\pi R_0} \quad (8)$$

By normalizing the value of the scattered field  $E_{sc}$  of (3) by the value provided by (8), the scattering coefficient  $\gamma$  is calculated by [1]:

$$\gamma = \frac{E_{sc}}{E_{sc0}} = \frac{1}{4L \cos \theta_i} \times \left( \left( q + \frac{pv_x}{v_z} \right) \times \int_{-L}^L \exp[iv_x x + iv_z f_r(x)] dx - \left\{ \frac{ip}{v_z} \exp[iv_x x + iv_z f_r(x)] \right\}_{-L}^L \right) \quad (9)$$

The first term in the parenthesis provides the most significant contribution to the scattering process, while the second term represents an edge effect, which can be considered negligible when  $L \gg \lambda$ , as assumed in this paper.

### 3. SIMULATION RESULTS

We concentrate on the backscattering of EM waves from rough fractal surfaces (e.g. monostatic SAR radar [9], [10]), i.e.  $\theta_s = -\theta_i$  at Fig. 1 and (4)–(7), and we plot the backscattering coefficient  $|\gamma(k)|$  (in magnitude). The surface is simulated as a zero-mean, band-limited fractal function, as in (1), and its roughness is controlled by the fractal dimension  $D$  [1], [3]. The backscattering coefficient  $|\gamma(k)|$  was calculated from (9) for a number of frequencies  $f_m = f_o + (m-1)\Delta f$ , where  $m = 1, 2, \dots, M$  and  $M$  is the number of frequencies,  $f_o$  is the carrier frequency,  $\Delta f = BW/M$  is the frequency step and  $BW$  is the bandwidth of the radar, i.e. 'stepped – frequency' transmitted radar waveform [9], [10]. Furthermore, in Figs. 2–5, below, the plots of  $|\gamma(k)|$  for angle of incidence  $\theta_i = 30^\circ$  are shown, while the values of the other parameters are  $BW=1\text{GHz}$ ,  $f_o = 10\text{GHz}$  (initial radar carrier frequency) and  $M = 200$  (i.e. 200 frequency steps in radar emitted stepped-frequency waveform).

As far as the simulated fractal surface is concerned, the frequency scaling parameter was set equal to

$b = 1.8$  while the number of tones was set equal to  $N = 6$  [1]. Moreover, the rms height of the surface was set equal to  $\sigma = 0.05\lambda$ ,  $\Lambda_0 = 10\lambda = 0.3$  m and the illuminated length of the rough surface along  $x$ -direction ('patch size') was chosen to be  $2L = 80\lambda$  (Fig. 1) in all calculations (so as  $2L \gg \Lambda_0$  and  $k\sigma < 1$ ), where  $\lambda = c/f_0$  [1], [18].

Furthermore, at the top left corner of each figure a sample plot of the roughness fractal function  $f_r(x)$  (1) is also shown.

The roughness of the simulated fractal surface (the fractal dimension  $D$ ) is increasing per image, e.g.  $D = 1.05$  (Fig. 2),  $D = 1.30$  (Fig. 3),  $D = 1.55$  (Fig. 4),  $D = 1.80$  (Fig. 5).

By observing Figs. 2–5, the following conclusion is made: as the value of the parameter  $D$  increases, i.e. as the roughness of the fractal surface increases, the emerging slope between the main lobe and the side lobes also increases.

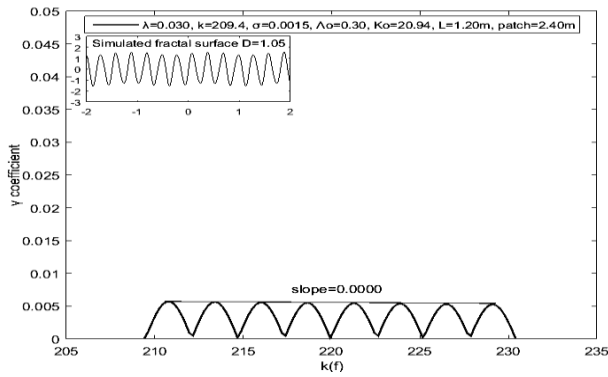


Fig. 2. Magnitude of backscattering coefficient  $|\gamma(k)|$ , as a function of the wavenumber  $k$ , for  $D = 1.05$ .

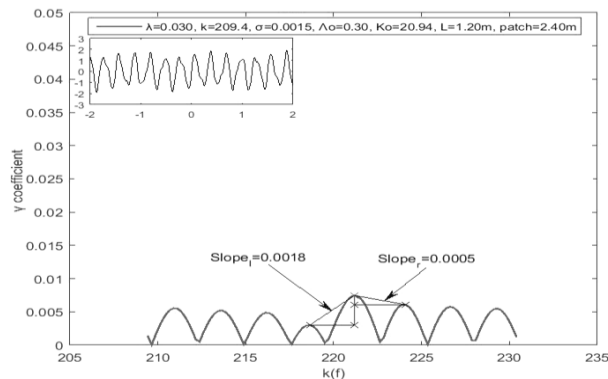


Fig. 3. Magnitude of  $|\gamma(k)|$  as a function of the wavenumber  $k$ , for  $D = 1.30$ .

Therefore, it becomes clear in our simulations that the roughness of the fractal surface can be characterized by the mean slope between the main lobe of

function  $|\gamma(k)|$  and the two sidelobes, adjacent to the main lobe (see Figs. 2–5).

In Table 1, below, the relation between the fractal dimension  $D$  and the slope calculated from each graph is shown. The slope is equal to  $|\Delta\gamma|/|\Delta k|$ , where  $\Delta\gamma$  represents the amplitude difference between the peak of the main lobe and the peak of the first side lobe, while  $\Delta k$  represents the difference of the wavenumbers where these peaks occur.

Table 1. Fractal dimension  $D$  and the resulting slope calculations

D	Left slope calculations			Right slope calculations		
	$\Delta\gamma$	$\Delta k$	slope	$\Delta\gamma$	$\Delta k$	slope
1.05	0.0000	0.00	0.0000	0.0000	2.62	0.0000
1.30	0.0044	2.51	0.0018	0.0014	2.93	0.0005
1.55	0.0285	5.03	0.0057	0.0202	3.77	0.0054
1.80	0.0883	3.98	0.0222	0.0819	3.77	0.0217

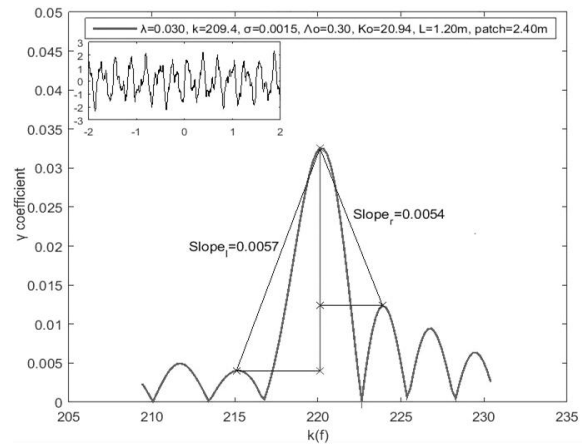


Fig. 4. Magnitude of  $|\gamma(k)|$  as a function of the wavenumber  $k$ , for  $D = 1.55$ .

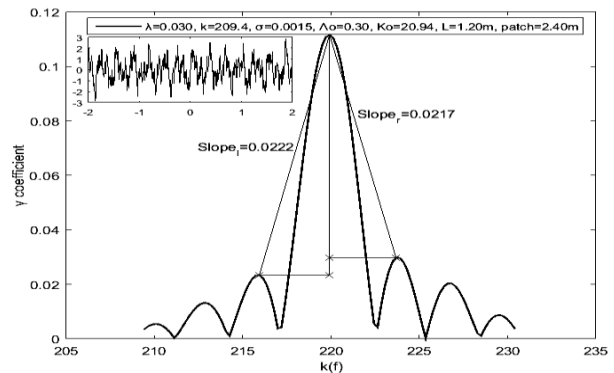


Fig. 5. Magnitude of  $|\gamma(k)|$  as a function of the wavenumber  $k$ , for  $D = 1.80$ .

If the radar bandwidth decreases, then the information provided by the backscattered signal-wave-

number plots, of the type provided above, is not always enough in order to draw safe conclusions regarding the roughness (fractal dimension) of the surface. In other words, the bandwidth for our proposed method of surface characterization from backscattered radar data must be sufficiently large (at least 5% of the carrier frequency  $f_o$ ), in order that the information contained in the plots of Figs. 2–5 to be observable and measurable.

In order to study further the relation between the surface fractal dimension  $D$  and the slopes of the scattering coefficient  $|\gamma(k)|$ , some additional simulations have been performed, as follows. The  $|\gamma(k)|$  was calculated sequentially for different values of fractal dimension  $D$ ,  $D = 1.05, 1.10, 1.15, \dots, 1.85, 1.90$  (i.e. here for 18 subsequent values of parameter  $D$ ), while the rest of the parameters used in these simulations remained the same as in Figs. 2–5. The left and right slope calculations of  $|\gamma(k)|$ , corresponding to each value of  $D$ , were averaged, thus creating one average slope calculation of  $|\gamma(k)|$  for each value of  $D$ .

Furthermore, in order also to demonstrate the robustness of our proposed method, we inserted in (1) a uniformly distributed random phase variable  $\varphi_n$  in the interval  $[0, 2\pi]$ , for every new surface simulation run, namely for every different  $D$  value. The calculation results, after 10 simulations for each  $D$  value, are presented in Fig. 6, below.

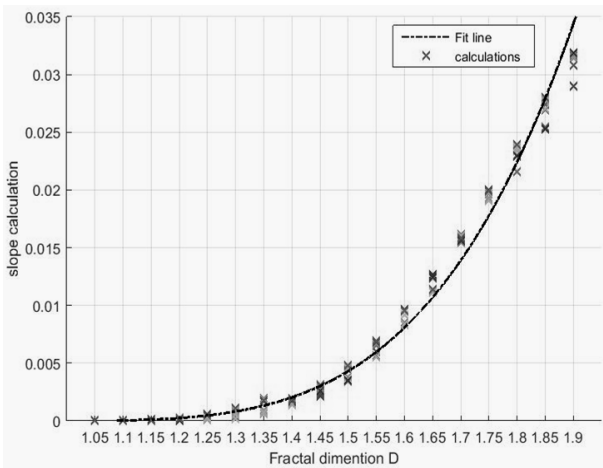


Fig. 6. Average slope' of the  $|\gamma(k)|$  vs. value of the surface fractal dimension  $D$ .

By 'inverting' the data (slope calculations and fitting curve) provided in Fig. 6, the plots of Fig. 7 are provided, where in this case the surface fractal dimension  $D$  is plotted as a function of the 'slope calculations' of the scattering coefficient  $|\gamma(k)|$ .

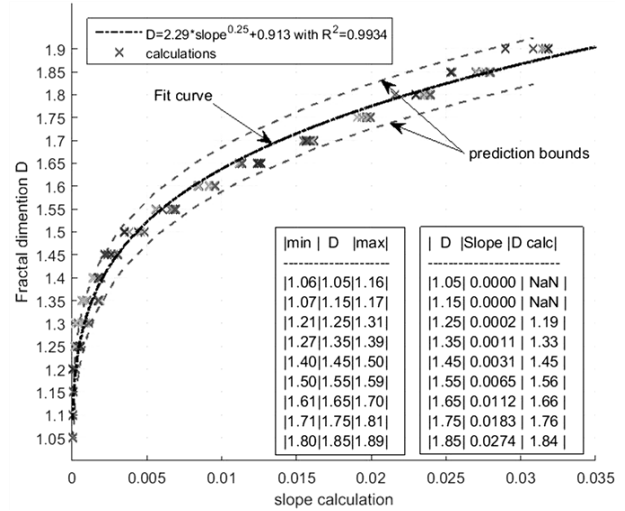


Fig. 7. Value of surface fractal dimension  $D$  vs. 'slope calculation' of  $|\gamma(k)|$ .

In Fig. 7 an analytical expression between the 'slope calculation' and the surface fractal dimension  $D$  has been calculated numerically by 'curve fitting'. Namely, it was found here that an excellent curve fitting exists if the fractal dimension  $D$  follows the relation  $D = a * slope^b + c$ . In Fig. 7 we plot the fit curve by using the following coefficients:  $a = 2.29$ ,  $b = 0.25$ ,  $c = 0.913$ , and as a measure of fit to our calculations we use 'R-square criterion for curve fitting', which, for the above simulations, yielded the value  $R^2 = 0.9934$ . We plot also the prediction bounds for the fitted curve. The prediction is based on the existing fit to our simulation calculations by using a 90% 'probability of occurrence'. Based on the fitted curve model and the prediction bounds for the fitted curve, Tables 2 and 3 below are presented, as follows :

TABLE 2

ESTIMATION OF  $D_{CALC}$   
 $D_{calc} = 2.29 * slope^{1/4} + 0.913$

$D$	Slope	$D_{calc}$
1.05	0.0000	none
1.15	0.0000	none
1.25	0.0002	1.19
1.35	0.0011	1.33
1.45	0.0031	1.45
1.55	0.0065	1.56
1.65	0.0112	1.66
1.75	0.0183	1.76
1.85	0.0274	1.84

TABLE 3

$D_{CALC}$  PREDICTION INTERVAL  
 USING PREDICTION BOUNDS

$D_{calc}$ lower	$D$	$D_{calc}$ upper
1.06	1.05	1.16
1.07	1.15	1.17
1.21	1.25	1.31
1.27	1.35	1.39
1.40	1.45	1.50
1.50	1.55	1.59
1.61	1.65	1.70
1.71	1.75	1.81
1.80	1.85	1.89

Table 2 presents the value  $D$  that was used for the simulation, the slope that was calculated from this simulation and the  $D_{\text{calc}}$  value, which was calculated using our model. For  $D = 1.05$  to  $D = 1.15$ , namely for almost smooth surfaces, the slope is almost zero and for these cases our model could not establish a clear  $D_{\text{calc}}$  value. However for rough surfaces with  $D > 1.25$ , our proposed model proved to predict the fractal dimension  $D$  of the rough surface with excellent accuracy (see Table 2).

The accurate results of Table 2 gave us the motivation to stress the robustness of our method, by adding random phases  $\varphi_n$  to the rough surface modeling function (1), for each surface simulation. The variability of slope calculations for each value of  $D$  in Figs. 7, 8 depicts this added surface randomness. Table 3 presents the prediction intervals for the  $D_{\text{calc}}$  estimation. This interval indicates that for any new observation from a fractal surface, there exists 90% probability that the value of the fractal dimension of the surface lies within the prediction bounds of this Table 3. This Table demonstrates the fact that our proposed method is accurate and robust enough to characterize a rough fractal surface from backscattered radar data, and also provides a bound estimation for the fractal dimension  $D$  of this surface.

Note that if the angle of incidence is  $\theta_i \approx \pi/2$  (i.e. EM wave incidence almost parallel to the rough surface, see Fig. 1), and since in this paper we are interested only for the backscatter case, i.e.  $\theta_s = -\theta_i$ , from (7) it follows that in this case  $\nu_z \approx 0$ , and from (9) we see that our method is *not* applicable in this special case, since the scattering coefficient  $|\gamma(k)|$  can not be computed. Summarizing, our proposed method for characterizing a rough fractal surface provides reliable results for appropriate values of radar bandwidth, surface 'patch size' [19] and angle of incidence.

Furthermore in this paper, and in order to examine whether our method could have a practical implementation in a noisy radar environment, we add AWGN noise in  $\gamma(k)$ . We use eq. (10), below, for calculating the power level  $P(\gamma)$  of signal  $\gamma(k)$ , and eq. (11) for calculating the noise level  $N(\gamma)$  for a given  $SNR$  value.

$$P(\gamma) = \frac{1}{n} \sum |\gamma(m)|^2 \quad (10)$$

$$N(\gamma) = \frac{P(\gamma)}{SNR} \quad (11)$$

$$\gamma_{\text{noisy}} = \gamma + \sqrt{\frac{P(\gamma)}{SNR}} \text{Norm}(0,1) \quad (12)$$

where  $m=1$  to  $n$  in the summation of eq. (10), above. The  $\gamma_{\text{noisy}}$  in (12) represents a  $\gamma(k)$  signal that exhibits a certain  $SNR$  value using a Gaussian distribution with specific noise level.

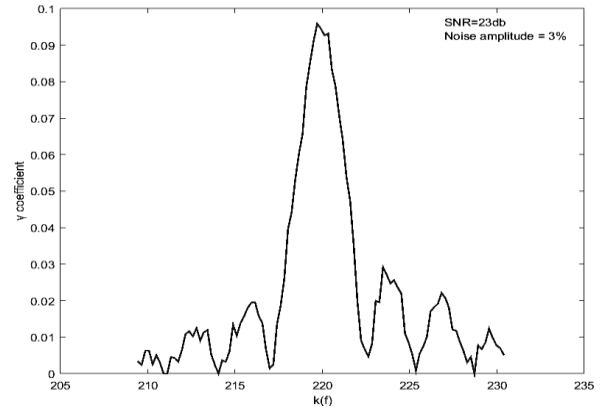


Fig. 8.  $\gamma(k)$  with SNR 23db inserts a noise amplitude 3% of  $|\gamma(k)|$  max amplitude.

From figure 8 it is obvious that a signal  $\gamma(k)$  exhibiting high  $SNR=23\text{db}$  does not affect our proposed method.

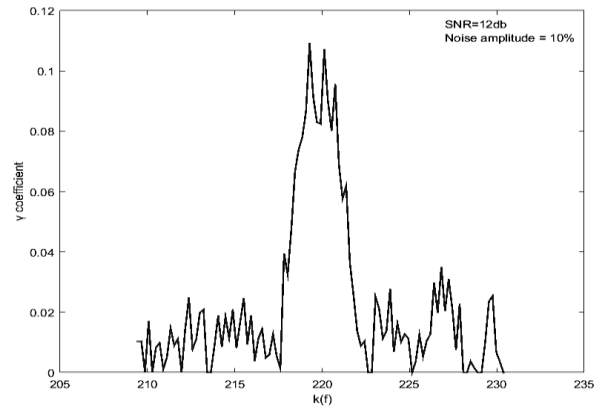


Fig. 9.  $\gamma(k)$  with SNR 12db inserts a noise amplitude 10% of  $|\gamma(k)|$  max amplitude.

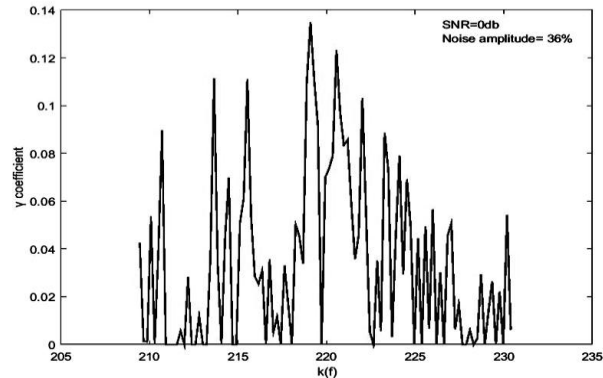


Fig. 10.  $\gamma(k)$  with SNR 0db inserts a noise amplitude 36% of  $|\gamma(k)|$  max amplitude.

On the contrary a signal  $\gamma(k)$  exhibiting low  $SNR=0db$  (signal=noise), as demonstrated in figure 10, can totally suppress sidelobes and cancel our proposed method, if no additional noise suppression technique is applied.

Further to the above, there are several techniques that can be used to improve  $SNR$  and make our method useful for lower  $SNR$  values. Choosing the appropriate technique depends on what kind of noise interferes with the signal. In case of AWGN, it is possible to enhance the  $SNR$  by averaging measurements. Theory suggests that the noise goes down about as the square root of the number of averaged samples. Here we propose averaging over  $N$  successive bursts.

In figure 11 we obtain the improvement of figure 9 after an averaging of 25 samples ( $N=25$  bursts). In figure 12 we obtain the improvement of figure 10 after averaging of 100 samples.

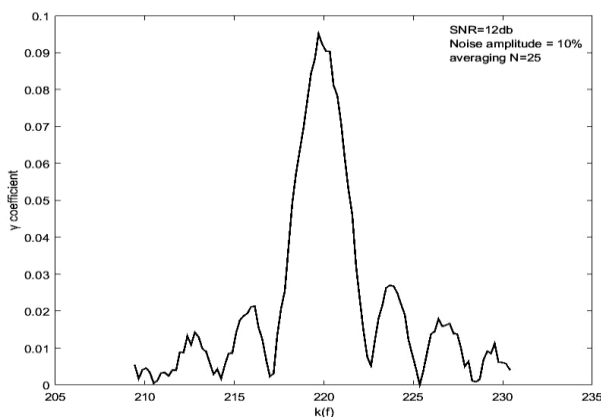


Fig. 11.  $\gamma(k)$  with  $SNR$  12db after  $N=25$  bursts averaging

It is obvious that the number  $N$  of bursts that are needed for having a useful signal of  $\gamma(k)$  depends on the  $SNR$  value, namely noise level. The only trade-off is that when number of  $N$  is increased, it is possible the target (e.g. sea surface) to look as a 'different target' during successive bursts. So the number of bursts is only limited by the rate of change of the target geometry.

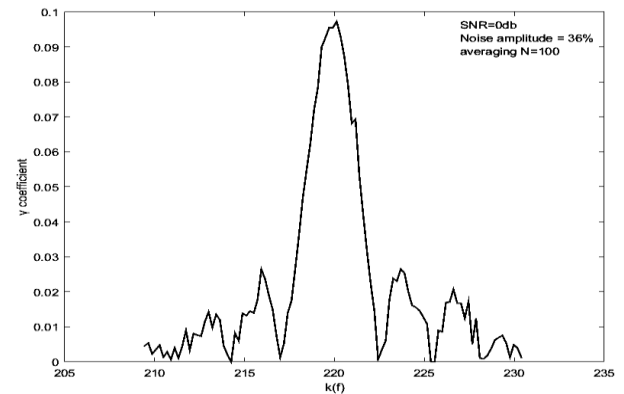


Fig. 12.  $\gamma$ -signal with  $SNR$  0db after  $N=100$  bursts averaging

#### 4. CONCLUSION

In this paper, a novel method is presented for the characterization of rough fractal surfaces from backscattered radar data of *sufficient bandwidth* [9], [10]. As resulted from the plots of the backscattered signal magnitude as a function of the wavenumber (frequency, therefore a '*spectral method*') of the incident EM wave, as the roughness of the fractal surface increases, then the observed slope between the main lobe and the side lobes also increases. Moreover, the fractal dimension of the surface can be estimated by the average slope of backscattering coefficient  $|\gamma(k)|$ . Furthermore, the value of the available radar bandwidth is crucial and must be sufficiently large, for correct rough surface characterization. Finally, we prove that our method is useful even in a noisy radar environment which exhibits  $\gamma(k)$  with relatively low  $SNR$ . It is only a matter of selecting the appropriate averaging number of bursts in order to enhance  $SNR$  of signal  $\gamma(k)$ .

#### ACKNOWLEDGMENTS

The authors would like to express their sincere thanks to Prof. N. Ampilova and Prof. I. Soloviev, Faculty of Mathematics and Mechanics, St. Petersburg State University, Russia, for interesting discussions and suggestions of theirs, which stimulated this research at the various stages of its implementation.

## References

- [1] D. L. Jaggard, X. Sun, "Scattering from fractally corrugated surfaces", *Journal of the Optical Society of America A*, Vol. 7, No 6, pp. 1131-1139, 1990.
- [2] P. Beckmann, A. Spizzichino, *The Scattering of electromagnetic waves from rough surfaces*, Artech House Inc., 1987.
- [3] D. L. Jaggard, A.D. Jaggard, P. Frangos, "Fractal electrodynamics: surfaces and superlattices", in *Frontiers in Electromagnetics*, Edited by Douglas Werner and Raj Mittra, IEEE Press, 2000, pp. 1-47.
- [4] F. Berizzi, E. Dalle Mese, G. Pinelli, "One dimensional fractal model of the sea surface", *IEEE Proc. Radar Sonar Navig.*, Vol. 146, No 1, pp. 55-64, 1999.
- [5] A. K. Sultan – Salem, G.L. Tyler, "Validity of the Kirchhoff approximation for electromagnetic wave scattering from fractal surfaces", *IEEE Trans. Geosc. Rem. Sensing*, Vol. 42, No. 9, pp. 1860-1870, 2004.
- [6] M. F. Chen, A. K. Fung, "A numerical study of the regions of validity of the Kirchhoff and small perturbation rough surface scattering models", *Radio Science*, Vol. 23, pp. 163 – 170, 1988.
- [7] E. Jakeman, "Scattering by fractals", in *Fractals in Physics*, pp. 55-60, 1986.
- [8] N. Ampilova and I. Soloviev, "On digital image segmentation based on fractal and multifractal methods", *CEMA'15 Conference Proceedings*, pp. 14-17, Sofia, Bulgaria, 2015.
- [9] A. Malamou, A. Karakasiliotis, E. Kallitsis, G. Boulidakis, P. Frangos, 'Application of a fully automatic autofocus algorithm for post – processing of synthetic aperture radar images based on image entropy minimization', *Electronics and Electrical Engineering Journal*, Vol. 19, No. 6, pp. 95 – 98, 2013.
- [10] A. Malamou, C. Pandis, P. Frangos, P. Stefanias, A. Karakasiliotis, D. Kodokostas, "Application of the modified fractal signature method for terrain classification from synthetic aperture radar images", *Electronics and Electrical Engineering Journal*, Vol. 20, No. 6, pp. 118–121, 2014.
- [11] S. Savaidis, P. Frangos, D. L. Jaggard and K. Hizanidis, "Scattering from fractally corrugated surfaces : an exact approach", *Optics Letters*, Vol. 20, No. 23, pp. 2357-2359, 1995.
- [12] S. Savaidis, P. Frangos, D. L. Jaggard and K. Hizanidis, "Scattering from fractally corrugated surfaces using the extended boundary condition method", *Journal of the Optical Society of America A*, Vol. 14, No. 2, pp. 475-485, 1997.
- [13] D. L. Jaggard, X. Sun, "Fractal surface scattering: a generalized Rayleigh solution", *Journal of Applied Physics*, Vol. 68, No 11, pp. 5456-5462, 1990.
- [14] M. F. Chen, A. K. Fung, "A numerical study of the regions of validity of the Kirchhoff and small-perturbation rough surface scattering models", *Radio Science*, Vol. 23, pp. 163-170, 1988.
- [15] E. I. Thorsos, "The validity of the Kirchhoff approximation for rough surface scattering using a Gaussian roughness spectrum", *Journal of Acoustical Society of America*, Vol. 83, No 11, pp. 78-92, 1988.
- [16] J. M. Soto-Crespo, M. Nieto-Vesperinas, "Electromagnetic scattering from very rough random surfaces and deep reflection gratings", *Journal of the Optical Society of America A*, Vol. 6, pp. 367-384, 1989.
- [17] D. L. Jaggard, Y. Kim, "Diffraction by bandlimited fractal screens", *Journal of the Optical Society of America A*, Vol. 4, pp. 1055-1062, 1987.
- [18] J. Fikioris, *Introduction to Antenna Theory and Propagation of Electromagnetic Waves*, pp. 155-156, National Technical University of Athens (NTUA), Athens, Greece, 1982.
- [19] A. Kotopoulos, A. Malamou, G. Pouraimis, E. Kallitsis and P. Frangos, "Characterization of rough fractal surfaces from backscattered radar data", 'Electronics and Electrical Engineering' Journal, accepted April 2016.